https://rbgeomorfologia.org.br/
*ISSN 2236-5664*

**Revista Brasileira de Geomorfologia**

v. 26, nº 2 (2025)

http://dx.doi.org/10.20502/rbgeomorfologia.v26i2.2647

*Artigo de Pesquisa*

# Hydrosedimentary dynamics and morphological features of a rocky channel bend: Piquiri River, PR, Brazil

## *Dinâmica hidrossedimentar e caracterização morfológica de uma curva de canal rochoso: Rio Piquiri, PR, Brasil*

**Altair Bennert [1], José Cândido Stevaux [2], Geovani da Silva Lima[3], Isabel Terezinha Leli[4], Ericson Hideki Hayakawa[5]**

[1] Western Paraná State University, Unioeste –Graduate Program in Geography,Marechal Cândido Rondon, PR, Brazil. E-mail. bennert.geo@gmail.com
ORCID: https://orcid.org/ 0000-0001-8230-2288
[2] Federal University of Mato Grosso do Sul -UFMS –Graduate Program in Geography, Três Lagoas,MS, Brazil. E-mail. josecstevaux@gmail.com
ORCID: https://orcid.org/ 0000-0001-6136-2556
[3] Western Paraná State University, Unioeste –Graduate in Geography,Marechal Cândido Rondon, PR, Brazil. E-mail. geovani_lima17@outlook.com
ORCID: https://orcid.org/ 0009-0004-2531-787X
[4] Federal University of Mato Grosso do Sul -UFMS –Graduate Program in Geography, Três Lagoas,MS, Brazil. E-mail. isabeltleli@gmail.com
ORCID: https://orcid.org/0000-0002-4344-3739
[5] Western Paraná State University, Unioeste –Graduate Program in Geography,Marechal Cândido Rondon, PR, Brazil. E-mail. ericson.hayakawa@unioeste.br
ORCID: https://orcid.org/ 0000-0003-1342-1659

Recebido: 14/11/2024; Aceito: 31/03/2025; Publicado: 12/04/2025

**Abstract:** The size and geometry of alluvial river bends are a result of the stream power and the sediment load. However, the efficiency of these variables is not the same in rivers over rocky substrates. Considering the hypothesis that a channel bend influences the flow dynamics and characterizes specific flow zone conditions, bed morphology, and sediment load distribution, the objective of this study is to characterize these variables in a rocky-bottom controlled bend of the Piquiri River, PR, Southern Brazil. The methods used for this were: a) Field data collection (bottom and suspended sediments, bathymetric Esurveys, and flow discharge and velocity); b) echosounder and ADCP data were processed by the ArcGis 10.4 and VMT (Velocity Mapping Toolbox) software; and c) Laboratory procedure (quantification of suspended and bottom sediment). The results demonstrate that the bottom morphology and channel curvature influence the depth variation, highlighting the increase in depth in the downstream section of the bend, as well as in the flow distribution and velocity with the generation of helical cells in the channel bend zone. The concentration of suspended sediment varies, both from upstream to downstream, as well as at different depths, being, however, significantly higher downstream of the bend. These results denote great importance in understanding the dynamics and flow processes in channel bends with rocky beds, with emphasis on the behavior of the flow with different pressure gradients.

**Keywords:** Morphology, helical movement, sediments.

**Resumo:** O tamanho e a geometria das curvas de rios aluviais são resultado da potência do canal e também da carga sedimentar do sistema. Entretanto, é importante ressaltar que a eficiência dessas variáveis não é a mesma em rios com substrato rochoso. Considerando a hipótese de que uma curva de canal influencia a dinâmica do fluxo e caracteriza condições específicas das zonas de fluxo, morfologia do leito e distribuição da carga sedimentar, o objetivo deste estudo é caracterizar o comportamento do fluxo, a morfologia do leito e quantificar o sedimento em suspensão e de fundo em uma curva do rio Piquiri, PR. Para tanto, foram utilizados os métodos: a) Coleta de dados de campo (sedimentos, batimetria, medição de vazão e velocidade de escoamento); b) Processamento dos dados do ecobatímetro e do ADCP com os programas ArcGis 10.4 e VMT (Velocity Mapping Toolbox); e c) Procedimento laboratorial (quantificação de sedimento em suspensão e de fundo). Os resultados demonstram que a morfologia do fundo e a curvatura do canal influenciam na variação da profundidade, destacando-se o aumento da profundidade no trecho a jusante da curva, bem como no comportamento e distribuição da velocidade do escoamento no canal com geração de células helicoidais na zona de curvatura do canal. A concentração de sedimento em suspensão varia, tanto de montante para jusante, quanto em diferentes profundidades, sendo, no entanto, significativamente maior a jusante da curva. Esses resultados denotam grande importância na compreensão da dinâmica e dos processos de escoamento em curvas de canal com leitos rochosos, com ênfase no comportamento do escoamento com diferentes gradientes de pressão.

**Palavras-chave:** morfologia, movimento helicoidal, sedimentos.

## 1. Introduction

Studies on the dynamics and structuring of water and sediment flow in river channel bends began in the mid-20th century with the work of Dury (1953), Balek and Kolar (1959), Bagnold (1960), Leopold and Wolman (1957, 1960), Leopold et al. (1964), among others. From the beginning of the 21st century, with the development of new technologies, especially the georeferenced ecobathymeter and the Acoustic Doppler Current Profiler (ADCP), there has been considerable progress, particularly in determining flow structure, bed morphology, and sediment transport.

Precursor studies of meandering rivers covered various topics, such as the temporal morphological alteration of curves in the Karan River (YOUSEFI et al., 2016); the evolution of meanders due to the influence of secondary flow (CHEN; TANG, 2012); combined analysis of field data, remote sensing, and computational modeling (KASVI et al., 2015); the influence of sediment load composition (KAYVANTASH et al., 2017; TIRON et al., 2009); and the influence of plant remains in small meandering channels (DANIELS; RHODES, 2003). A rich collection of studies on various topics related to meandering channels can be found in the special volume "Meandering Channels" in Geomorphology, edited by Güneralp et al. (2012).

However, most of these studies were developed in alluvial rivers, mainly those with intense channel migration and bar formation. Rocky rivers with curves controlled by lithostructure have not received the same attention, and the few related articles are about mountain channel rivers with high loads of boulders and gravel associated with ephemeral high-energy flows (e.g. MILLER; CLUER, 1998; CENDERELLI; CLUER, 1998). The same has happened for South American rivers, whose studies have mostly focused on alluvial river curves. Luz et al. (2017) investigated the evolution of a meander of the Cuiabá River considering the relationship between flow structure and erosion of the concave bank that caused the "cut-off" in two years; Ramonell et al. (2007) measured changes in the sinuosity of the Bermejo River channel, Argentina, after the construction of a bridge; and Luz et al. (2020) presented the dynamics of a meandering confluence of the Paraguay and Cuiabá rivers.

Regarding the gap in studies on rocky bed river bends, Engel (2014), Stevaux, and Latrubesse (2017) emphasize the importance of understanding this type of channel and the processes involved in the development of predictive models of the dynamics and evolution of these forms. Thus, the objective of this study is to show the morphohydraulic relationships and the behavior of the sediment load transported (suspended and bed load) in an alluvial-rocky river bend.

This study was developed on a curve of an alluvial-rocky stretch of the Piquiri River, continuing the work of Bennert et al. (2023), thus enabling the aggregation and integration of more data and enriching the results. The lack of studies on curves of alluvial-rocky channels highlights the importance of this research in integrating, complementing, and providing support to other studies on the flow behavior and morphology of channels in rivers of this nature.

## 2. Study area Characterization

The Piquiri River originates at an altitude of 1,040 m in the Serra de São João, which is the boundary between the municipalities of Guarapuava and Turvo, PR, and flows for 485 km (LIMA et al., 2004) until its mouth on the left bank of the Paraná River, 15 km upstream from the city of Guaíra, PR. The section of the channel studied consists of a litho-structural curve of 40 degrees, with a length of 1.6 km to 3.0 km from the mouth. In this location, the river has a mixed condition due to the formation of a floodplain on the right bank, which is 1.8 km wide, and the left bank formed by basalt from the Serra Geral Formation. The floodplain exhibits a morphology composed of paleochannels, suggesting a progressive migration towards the left bank (Fig. 1).

The native vegetation of this area is the Submontane Seasonal Semideciduous Forest; however, due to exploitation, only a few local fragments remain (PAROLIN et al., 2010). The climate is predominantly of type Cfa (humid subtropical without a dry season), and the precipitation is less than 1,300 mm per year (BITTENCOURT, 1993). The average flow of the lower course of the Piquiri River is 505 $m^3/s$, as measured by the Balsa Santa Maria gauging station (64.830.000), with a 38-year historical series. The drainage basin of the Piquiri River covers 24,700 $km^2$ (LIMA et al., 2004), and its specific production of suspended sediment throughout the basin is classified as low to moderate (43 to 135 $t/km^2$/year), and the concentration of suspended sediment ranges from very low to moderate (46 to 140 mg $L^{-1}$) (LIMA et al., 2004).

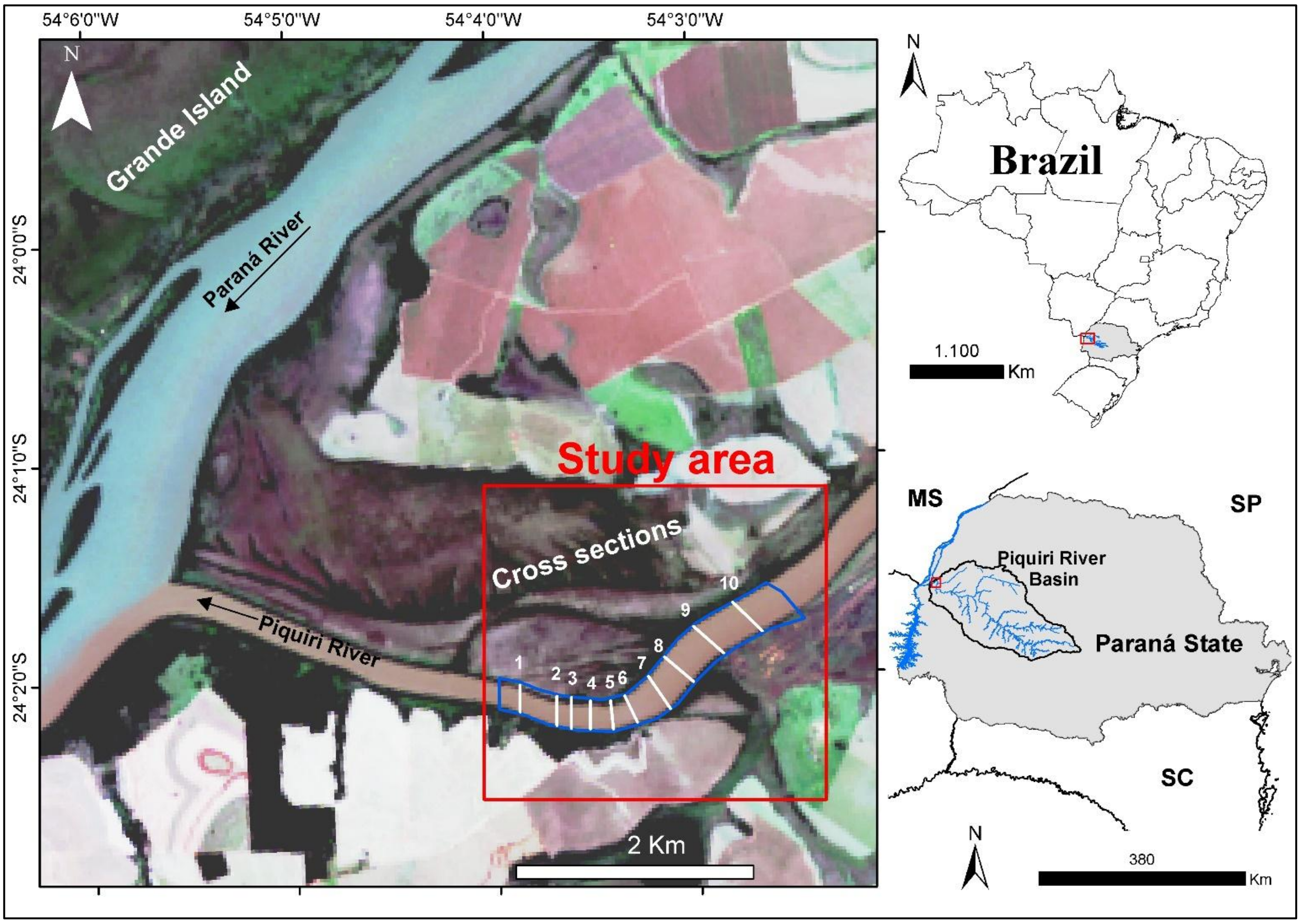


**Figure 1**. Section of the mouth of the Piquiri River into the Paraná River. Study area in the red rectangle. Numbers: studied sections. Landsat-8 image, OLI Sensor, date 08/06/2014.

## 3. Materials and Methods

The field survey was conducted from December 7 to 11, 2016, under average channel flow conditions (~500 $m^3/s$). Suspended and bed sediment samples were collected, bathymetry of the channel was performed, and flow rate, velocity, and flow direction were measured at 10 sections (Fig. 1). The stretch of the channel was segmented into three sectors: upstream of the bend (sections 7, 8, 9, 10), bend (sections 4, 5, 6), and downstream of the bend (sections 1, 2, 3).

Suspended sediment samples were collected at depths of 50 and 150 cm using a Van Dorn bottle, and for the bottom sediment, a modified van Veen grab was used.

The bathymetric survey was conducted using a georeferenced Furuno echosounder, model GP1650F, connected to a portable computer to record coordinates and depths (x, y, and z) using the Fugawi 4.5 software. The procedure consists of repeated cross-navigations between the banks and longitudinally covering the entire study area. Flow discharge, velocity, and acoustic response (backscatter) data were acquired by the ADCP (Acoustic Doppler Current Profiler) equipment, model River Ray Teledyne RDI (Thousand Oaks, CA), with a frequency of 600 kHz. The equipment is connected to a portable computer via the WinRiver II software.

The structural analysis of the area was based on the drainage alignment, the same method used by Souza Júnior et al. (2013) for the mouth of the Ivaí River.

### 3.1. Processing of bathymetric data and flow velocity

The data processed in the Fugawi 4.5 program were exported as a text file, organized in Excel software, and subsequently interpolated using the Ordinary Kriging procedure, with the bathymetric map created in ArcGIS 10.4. The ADCP data in ASCII format for each section were exported and processed in the VMT (Velocity Mapping Toolbox) program (PARSONS et al., 2013), which is based on Matlab and can be exported to files compatible with ArcGIS and Tecplot programs (PARSONS et al., 2013; ENGEL and JACKSON, 2016). Using the VMT program, the flow direction and velocity map was also created. The ASCII data for each section were converted and exported in Matlab (*.mat) format, which were accessed in VMT and processed together to generate the image. Through this software, the secondary flow in the vertical sections was also identified using Rozovskii's method (1957) (SZUPIANY et al., 2009).

### 3.2. Analysis of suspended and bed sediment

The concentration of suspended sediment was obtained by filtering a defined volume of collected water using Millipore filters (previously weighed dry) attached to a vacuum pump (ORFEO, 1995; LELI et al., 2010). Subsequently, the filters with the retained sediment were dried in an oven for 24 hours at 105º C for later weighing on a precision balance, with the difference between the initial and post-filtration filter weights corresponding to the total load. The filter was then placed in a muffle furnace for four hours at 480º C to burn the organic matter. Afterward, it was weighed again at room temperature to determine the concentration of suspended sediment without the organic matter. The suspended sediment results from each sample were then plotted in an Excel table with the corresponding depth and geographic coordinates. The statistical graphs were obtained from the Excel table and processed in the R program (RSTUDIO) with the ggplot2 package, which enabled the mapping of suspended sediment at different depths.

The distribution of suspended sediment concentration for each of the vertical profiles was obtained by correlating the "backscatter" signal (signal return intensity) from the ADCP (dB) with the measurement of suspended sediments collected at different depths in the field (DORNELLES, 2009; SZUPIANY et al., 2009; SZUPIANY et al., 2012; LATOSINSKI et al., 2014; WEIBEL et al., 2022). This method allowed for the identification of the sediment distribution in the study area.

The estimation of the bed material was obtained by sieving the dry material through a set of sieves with diameters of 16, 8, 4, 2, 1, 0.5, 0.25, 0.125, and 0.0625 mm (SUGUIO, 1973; CARVALHO, 1994).

## 4. Results and Discussions

### 4.1. Litho-structural analysis

The section of the Piquiri River curve is situated in small tilted blocks where its alluvial plain extends, with the channel migrating from the right bank upstream of the curve to the left bank downstream. Similarly, the lower course of the Pirapó River, a tributary of the Paranapanema River, has its course controlled by NE-SW and E-W structural lineaments (MINEROPAR, 2006). Such migrations, which occur in the Paraná River and its left-bank tributaries, are derived from litho-structural control (STEVAUX, 1994). Litho-structural control triggers the formation of a channel gradually filled with alluvial deposits, where the channel continuously migrates without altering the lateral dimensions of the channel (STEVAUX et al., 2019, 2021). This behavior has also been observed at the mouth of the Ivaí River (SOUZA JR. et al., 2013) and the Purus River, AM (LATRUBESSE; KALICKI, 2002).

Although limited to the Piquiri River end section, the mapping of relief and drainage lineaments reveals a strong litho-structural conditioning in the channel layout (Figs. 1 and 2), with lineaments in the NE-W and WNW-ESE directions closely aligned with the general trend mentioned above (Fig. 2 C and D). This is the same system in the Third Paraná Plateau, which develops similarly in the basaltic terrains of the Serra Geral Formation as in the arenaceous terrains of the Caiuá Formation. The same lineaments are also observed at the mouth of the Ivaí River (SOUZA JR. et al., 2013; FRANCO et al., 2008) and Paranapanema (PAES et al., 2008; STEVAUX et al., 2009).

Regionally, the most significant trends are in the N-S, NNW-SSE, and NE-SW directions, followed by another in the WNW direction, which is more strictly associated with drainage lineaments. These lineaments are linked to regional WNW lineament systems (Tietê River, Paranapanema River, Alonzo River, Piquiri River, Iguaçu River, among others) that cross almost the entire eastern edge of the Paraná Sedimentary Basin, likely derived from the uplift of the Ponta Grossa dome (e.g., FULFARO et al., 1982; PIRES NETO et al., 1994). The Paraná River, on the other hand, flows over a NE-SW lineament resulting from a normal fault with tilting of the lowered block to the east, i.e., toward the left bank (MAACK, 1968; STEVAUX, 1994). This condition leads to the asymmetric development of the floodplain on the right bank and the channel being diverted oppositely toward a high bank, typically composed of basalts from the Serra Geral Formation or resistant sandstones from the Caiuá Formation. However, it is observed that channel control in smaller rivers can be established by lineaments of lesser magnitude, with the presence of lowered blocks that may or may not be tilted. Martinez et al. (2011) observed that curves of the Pirapó River (20 km from its mouth into the Paranapanema River) are controlled by blocks with tilting on both the left and right banks (Fig. 2 A and B).

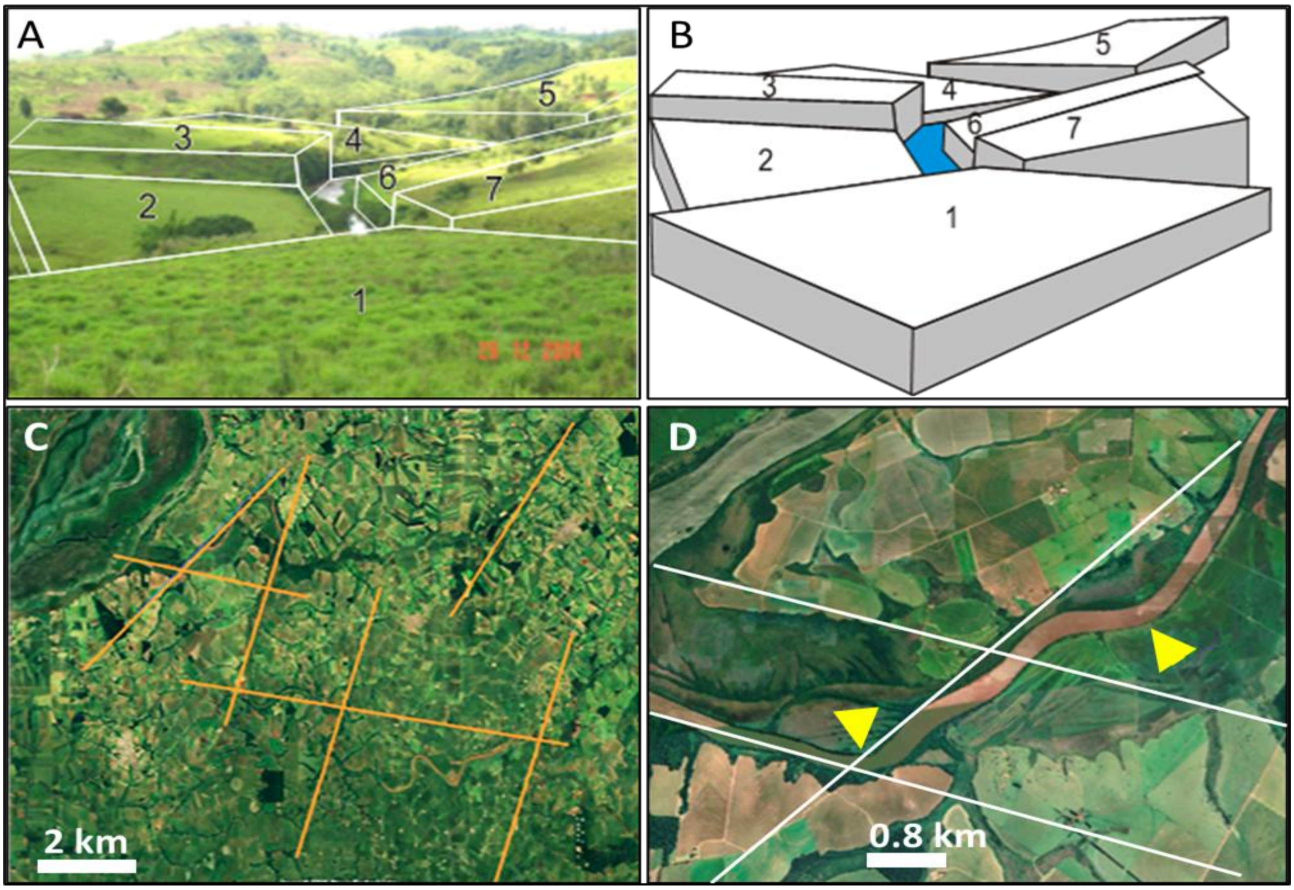


**Figure 2.** A: Curve of the Pirapó River under the control of small faults and tilted blocks; B: Block diagram of the same curve (Mod. MARTINEZ et al., 2011); C: Control of lineaments ~NE-SW and ~E-W in the lower course of the Piquiri River (Mod. MINEROPAR, 2006); D: Detail of the curve (yellow arrows indicate the dip of the tilted blocks).

### 4.2. Floodplain

As with other tributaries on the left bank of the Paraná River, typical of the sandstone-basalt plateau, the floodplain of the Piquiri River develops only in the lower section, closer to the mouth. This is also the case for the Ivaí and Paranapanema Rivers, which have a channel embedded directly over the bedrock, with no floodplain formation until near the mouth. Such a condition has been observed by Santos et al. (2008) and Souza Jr. et al. (2013), who suggest that the floodplain forms near the mouth due to the structural influence developed by the proximity of the Paraná River. The alluvial plain of the curve section is defined by a set of small faults that result in the formation of lowered blocks, creating space for the development of the floodplain. As reported in Latrubesse and Kalicki (2002), Stevaux (1994), and Leli and Stevaux (2021), regardless of block tilting, the channel, over its history, can migrate across the entire alluvial plain. In the case of larger rivers, such as the Paraná River, the deviation occurs for two reasons: a) neotectonic imposition (FORTES et al., 2005; STEVAUX, 1994), b) autogenic changes, such as channel abandonment due to sedimentation and slope leveling (LELI; STEVAUX, 2022). In the case of the Piquiri River, as well as the Ivaí River (SANTOS et al., 2022), the channel migration appears to be driven by autogenic factors, meaning that as the floodplain is filled, the channel advances laterally to both banks. This process remains active as long as hydrological and sedimentary conditions remain constant (TUROWSCKI et al., 2008; STEVAUX; LATRUBESSE, 2017). The curve section shows the channel asymmetrically diverted to the left bank, leaving a floodplain with at least two stages of development (Fig. 1).

Core samples from a small floodplain of the Piquiri River, 30 km upstream of the studied section, show a dominance of dark mud deposition with iron nodules, locally alternating with very fine, dark, muddy sand. These deposits have sedimentation rates of 0.3 to 0.5 mm year$^{-1}$, values similar to those found in similar environments in the Paraná River (STEVAUX; SOUZA, 2004; REMOR et al., 2015; LELI; STEVAUX, 2021).

### 4.3. Channel morphology

The section of the channel upstream of the curve has a depth ranging from 4 to 6 m (Fig. 3) and a width of about 300 m, with a trapezoidal cross-section and a relatively homogeneous bottom (Fig. 3, Tab. 1). The longitudinal profile shows an abrupt change in morphology and a sudden increase in channel depth at the curve location due to the formation of a 10 m "knickpoint" and an 11 m deep scour at the curve's apex near the concave bank (Fig. 3). The downstream section of the curve maintains asymmetry similar to that of the curve, with the thalweg shifting to the left bank (Fig. 3, Tab. 1).

The longitudinal profile of the riverbed shows two distinct levels, one upstream with a depth of around 4 m, and another downstream with a depth between 7 and 8 m, separated by the 10 m "knickpoint" at the curve (Fig. 3). Both the "knickpoint" and the "scour" were not generated exclusively by hydraulic processes but also by litho-structural imposition, which facilitated the release of blocks removed during periods of more energetic hydrology, as mentioned in other basaltic bed rivers (STEVAUX; LATRUBESSE, 2010; 2017). The system of orthogonal and hexagonal fractures in the basalt facilitates the block detachment mechanism ("quarrying"), which is one of the most common and efficient mechanisms for bedrock lowering (MILLER, 1991; WHIPPLE, 1998). Lima and Binda (2013) identified hydraulic quarrying as the primary mechanism for rivers over the basalt of the Serra Geral Formation in Paraná.

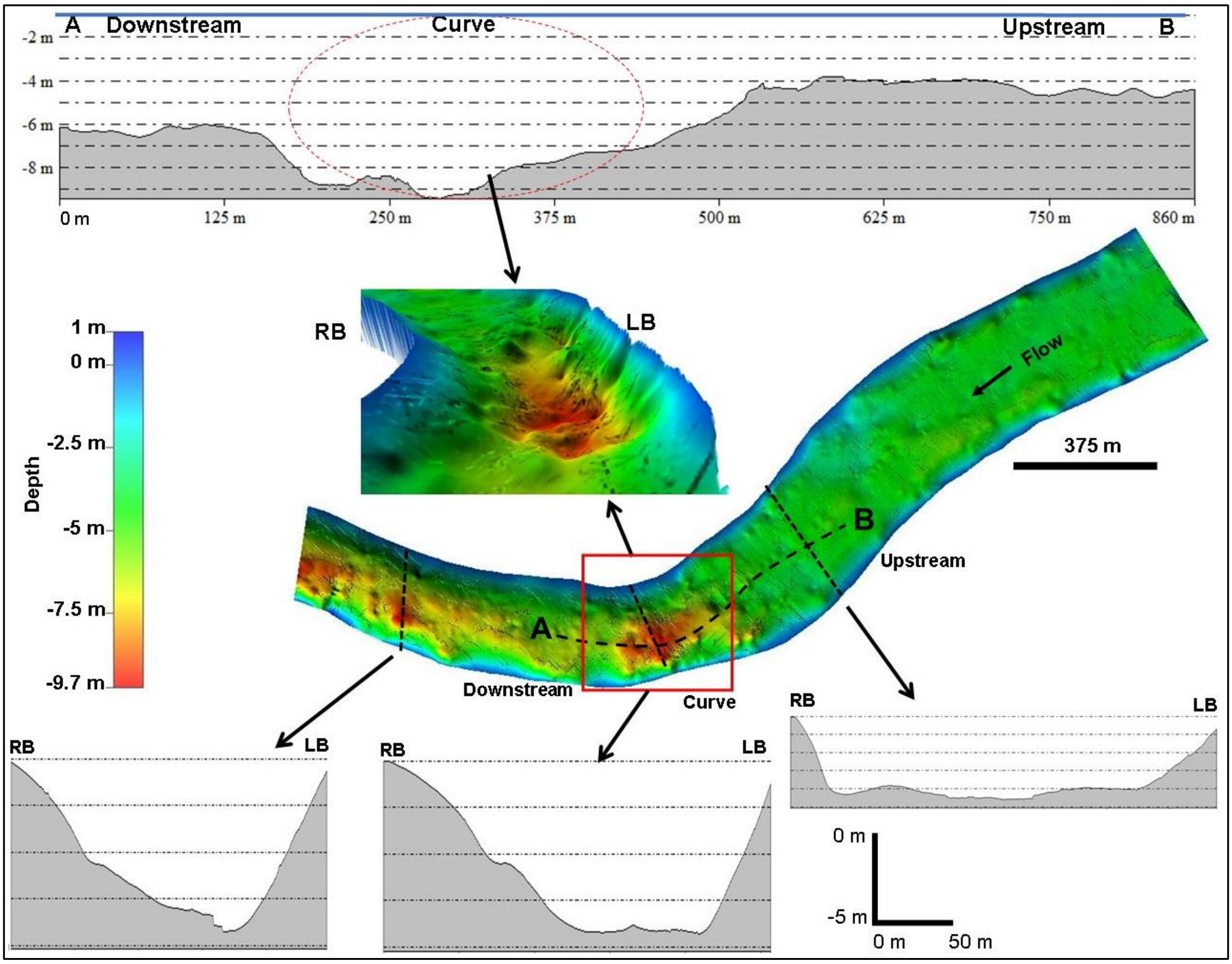


**Figure 3**. Bathymetry and variation of the channel depth.

## *4.4. Flow velocity and structuring*

The flow does not show significant variations along the sections of the reach, with an average velocity of 0.45 m $s^{-1}$. The flow direction changes behavior from upstream to downstream, with the flow upstream being almost parallel to the channel, with a slight deviation toward the left bank (S10, S9), increasing significantly as it reaches the curve (S8, S7, S6, S5, S4), with a continuous increase downstream (S1, S2, and 3). Similarly, the highest flow velocities are shifted toward the left bank of the channel in the downstream section (S10 to S7); however, they distribute homogeneously across the channel from the curve onward (S6 to S1) (Fig. 4). Consequently, the flow energy changes in these segments, with an average velocity of 0.40 m $s^{-1}$ in the upstream section, increasing to 0.547 m $s^{-1}$ downstream of the curve. The highest measured instantaneous velocity was 0.55 m $s^{-1}$ at S3. The slight increase in velocity downstream is driven by the "knickpoint," which causes an abrupt increase in the channel bed slope.

The instantaneous discharge values show a variation of up to 30%, with the lowest at S10 (548 $m^3$ $s^{-1}$) and the highest at S1 (768 $m^3$ $s^{-1}$). This condition is attributed to collection conditions, such as access to the banks or local variations in velocity (GUERRERO et al., 2016).

The deviation of the highest velocity zone toward the concave bank is a common process in channel curves due to the centrifugal displacement of the flow, which intensifies the formation of secondary cells that strengthen in the direction of this bank (STEVAUX; LATRUBESSE, 2017). The lower primary velocity in the channel curve area (Fig. 2) occurs due to the energy loss of the flow caused by the increased friction of the concave bank, as discussed by Konsoer et al. (2016). In this case, the flow energy is spent on the formation of vortices (MORISAWA, 1968). In the upstream section of the curve, the channel has a more regular bottom and secondary flow movements without the formation of large helical cells. This condition changes at the curve, where the bed presents greater depth and irregularity and an excavated area (Fig. 3), triggering both secondary flow and helical cells. The water flow at the curve site causes the super-elevation of the surface, creating a differential in the water pressure gradient and the formation of a cross-current toward the outer bank, which flows along the bed of the channel until the end of the curvature, resulting in the generation of helical cells (CHARLTON, 2007; ENGEL, 2014). The low hydraulic slope (0.00001) indicates the effect of damming by the Paraná River in reducing the specific power of the channel to less than 1 W $m^{-2}$ (measured by instantaneous discharges), also affecting the formation of helical cells downstream of the curve. Although the morphology and depth of the bed are maintained, the effect of the pressure gradient at the curve loses much of its action.

**Table 1** – Flow, average velocity, width, and average depth per transect during the sampling period.

| Transect | Flow (Q) ($m^3$ $s^{-1}$) | Average velocity (m $s^{-1}$) | Width (m) | Average depth (m) | Sector |
|---|---|---|---|---|---|
| **S 10** | 548.0 | 0.429 | 310 | 3.8 | Upstream |
| **S 9** | 546.1 | 0.392 | 311 | 4.5 | Upstream |
| **S 8** | 565.9 | 0.435 | 305 | 4.1 | Upstream |
| **S 7** | 564.4 | 0.460 | 302 | 3.9 | Upstream |
| **S 6** | 583.5 | 0.383 | 206 | 6.5 | Curve |
| **S 5** | 593.1 | 0.413 | 209 | 5.5 | Curve |
| **S 4** | 595.0 | 0.457 | 225 | 5.1 | Curve |
| **S 3** | 763.6 | 0.547 | 213 | 6.2 | Downstream |
| **S 2** | 769.9 | 0.530 | 206 | 7.1 | Downstream |
| **S 1** | 768.1 | 0.464 | 207 | 7.3 | Downstream |

The behavior of the helical secondary flow cells is distinct across the three sectors. The upstream sector (S10, S9, S8, S7) has the secondary flow distributed throughout the cross-section, but these consist of small and poorly defined elements, predominantly directed from the surface to the bed (Fig. 4). This condition changes at the channel curve (S6, S5, S4), where well-defined helical flow cells are present, and the flow is mostly clockwise (upstream-downstream direction). The displacement of the cells is predominantly from the right bank, meeting an anti-clockwise cell in deeper areas near the left bank in the curve sections. The flow moves from the surface to the bed toward the left bank, then returns near the bed in the opposite direction near the right bank. The downstream sector (S3, S2, S1) shows a restructuring of the flow with cells distributed throughout the section and a predominance of downward flows. However, the cells are smaller than those in the channel curve sector and occur near the left bank, with clockwise and anti-clockwise interactions at the meeting points of the cells.

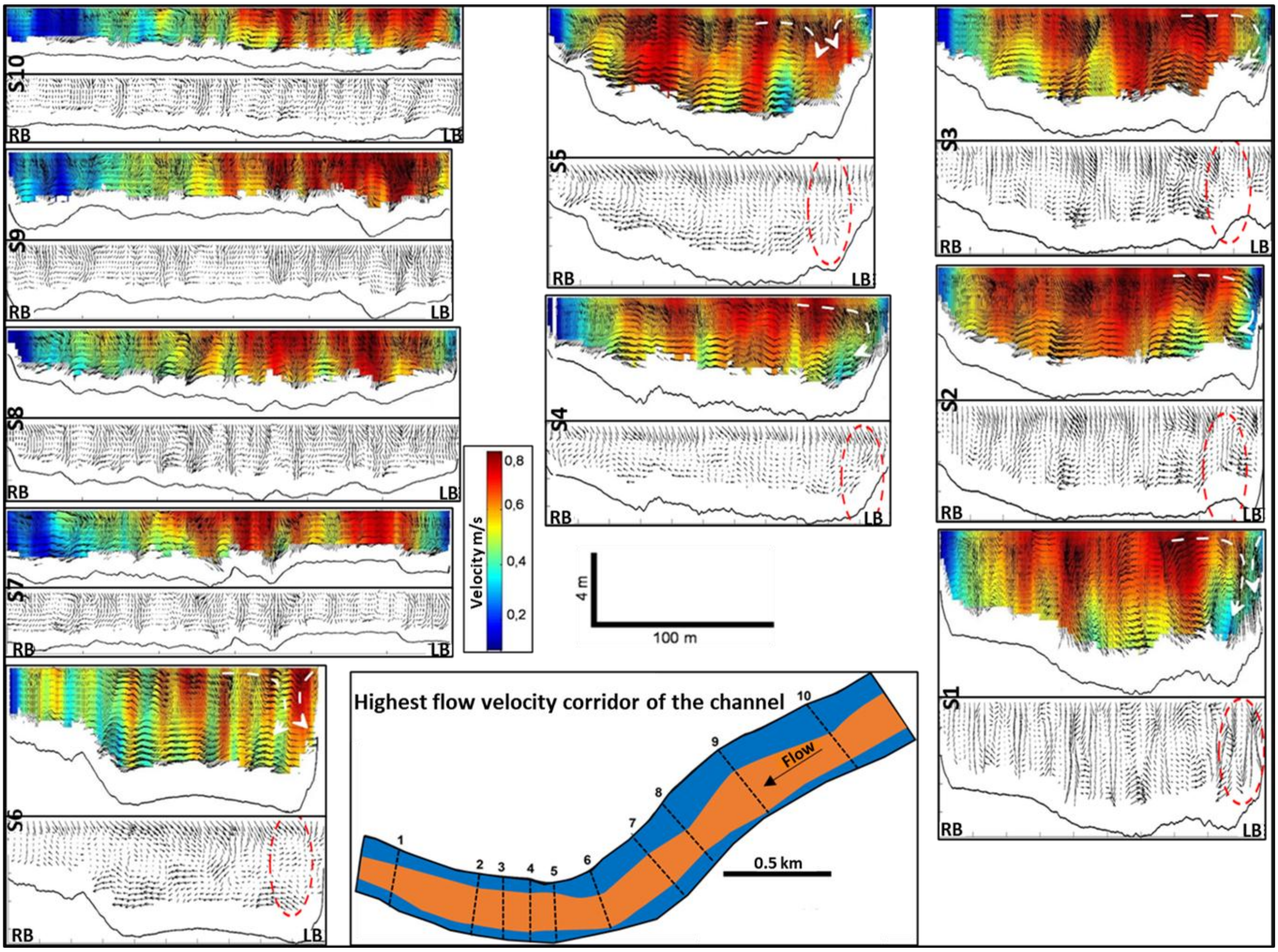


**Figure 4.** Distribution of flow velocity and secondary flow (black and white) with helical movement indicated by the arrows. Below: Highlight the river curve with the cross sections and the highest channel flow velocity corridor.

Although the rocky characteristic of the bed prevents the formation of meanders, in this case, the channel curvature imposed by the litho-structure has caused a dynamics flow similar to meandering channels, both in the influence of the curve on the flow due to the change in the water pressure gradient, and in the higher flow velocity on the left bank due to the shape of the bed and the presence of a point bar (Fig. 4). Similar results were observed by Engel (2014) and Konsoer et al. (2016).

The flow behavior of the Piquiri River in the section immediately downstream of the curve shows a general direction toward the left bank of the channel (BENNERT et al., 2023), with the authors attributing this condition to the effect of the studied curve on the flow and the restructuring of the downstream flow.

*4.5. Sediment transport*

The total suspended sediment concentration (Css) shows very similar values at both sampled depths. At 50 cm depth, it ranged from 15 to 45 mg $L^{-1}$, with the concentration predominantly between 25 and 35 mg $L^{-1}$, and an average of 30 mg $L^{-1}$. At 150 cm, it ranged from 20 to 47 mg $L^{-1}$, with an average of 31 mg $L^{-1}$. The same pattern was observed for the mineral sediment concentration (Cs), which ranged from 13 to 42 mg $L^{-1}$ at 50 cm, with an average of 18 mg $L^{-1}$, and from 15 to 37 mg $L^{-1}$ at 150 cm, with an average of 24 mg $L^{-1}$ (Fig. 5 A). The organic matter (OM) concentration reflected the same trend, ranging from 4 to 8 mg $L^{-1}$ with an average of 6 mg $L^{-1}$ at 50 cm, and from 5 to 9 mg $L^{-1}$ with an average of 7 mg $L^{-1}$ at 150 cm (Fig. 5 B).

However, longitudinally, the values of Css, Cs, and OM varied considerably, without showing a defined trend. The distribution of suspended load values found shows an unusual homogeneity in the case of alluvial rivers, where depth differentiation is more evident (SUGUIO; BIGARELLA, 1979). The irregularity of the rocky bed, with the occurrence of blocks of varying sizes, creates greater roughness and turbulence compared to alluvial rivers, where the channel is formed by homogeneous and smaller material (STEVAUX; LATRUBESSE, 2017).

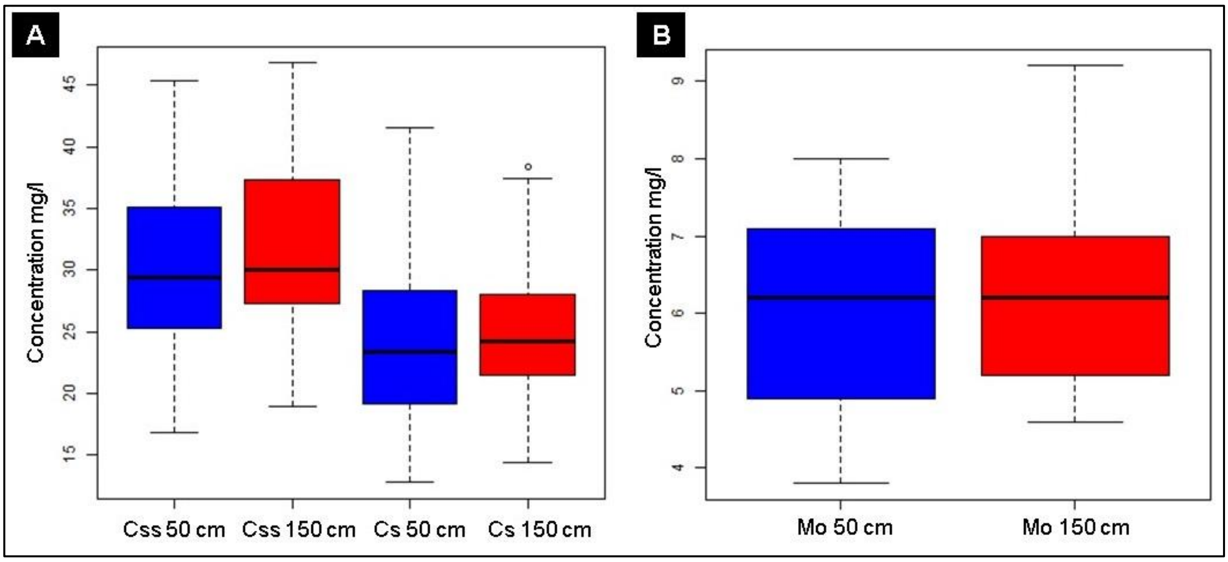


**Figure 5**. Concentration of total suspended sediment (Css), mineral (Cs), and organic matter (MO) at depths of 50 and 150 cm.

The spatial distribution of suspended sediments obtained by correlating the Backscatter (dB) values from the ADCP with the sediment concentration measurements (mg $L^{-1}$) resulted in a significant correlation with an $R^2$ close to 0.7 (Fig. 6), similar to the 0.8 found by Bennert et al. (2023) near the confluence with the Paraná River.

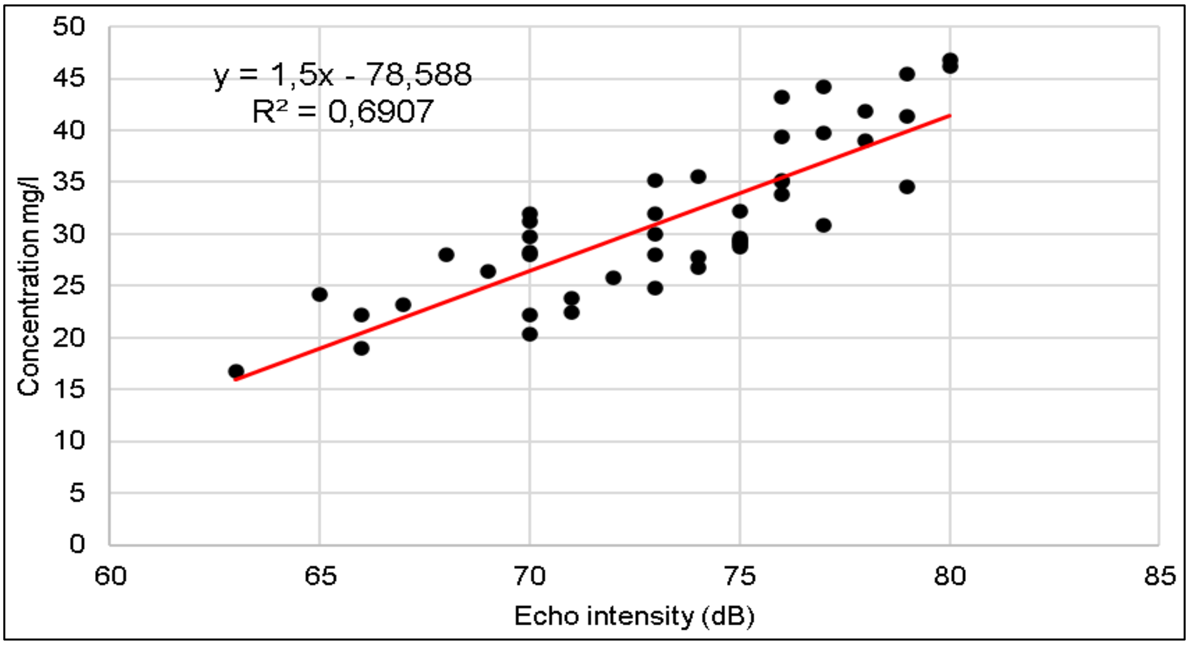


**Figure 6.** Correlation between Css and dB of the ten sections of the studied bend of the Piquiri River.

The distribution of suspended sediment concentration (Css) is more homogeneous in the upstream sections of the curve (S10, 9, 8, and 7), ranging from 26 to 41.4 mg $L^{-1}$, and downstream presents a greater variation with lower values at the surface and progressively higher values with increasing depth, ranging from 10.0 to 41.4 mg $L^{-1}$ (Fig. 7). The curve sections S6 and S5 show higher concentrations in the channel center at depths close to the bed, indicating the secondary flow influence and the helical movement on local sediment concentration.

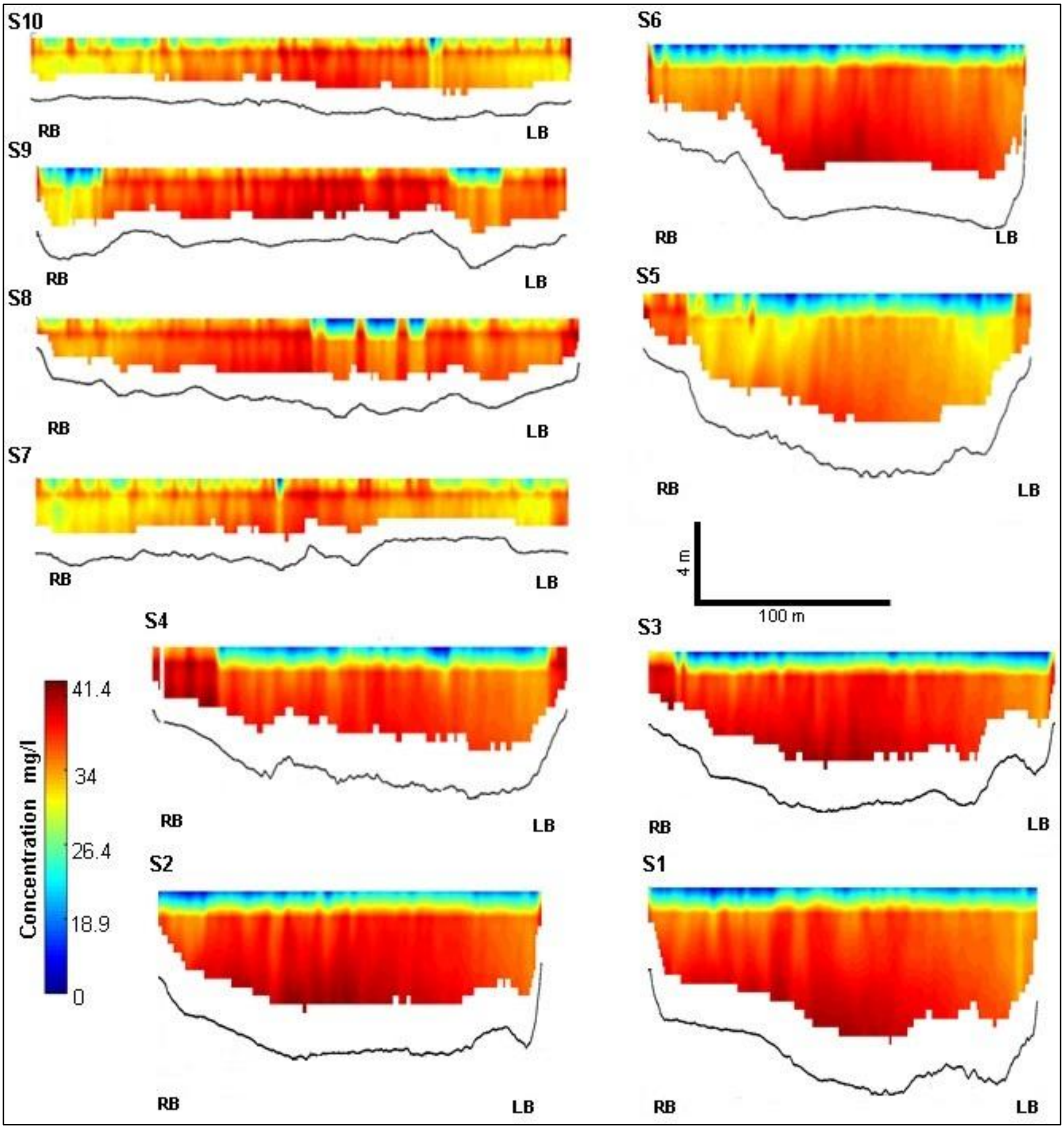


**Figure 7**. Distribution of sediments and organic matter at different depths.

The bed material is distributed throughout most of the section, except in the concave bank of the curve and the right bank (Fig. 8). The bed sediment upstream of the curve is predominantly composed of medium sand, followed by fine and very fine sand, maintaining the grain size of medium and fine sand with the presence of pebbles in the curve section. Downstream sections are dominated by medium sand and pebbles. During the field sampling period, the bed material was immobilized due to the low-flow energy condition. This condition indicates that the transport of this material occurs during the channel's flood periods, particularly during floods that do not coincide with those of the Paraná River, which imposes an increase in the system's energy.

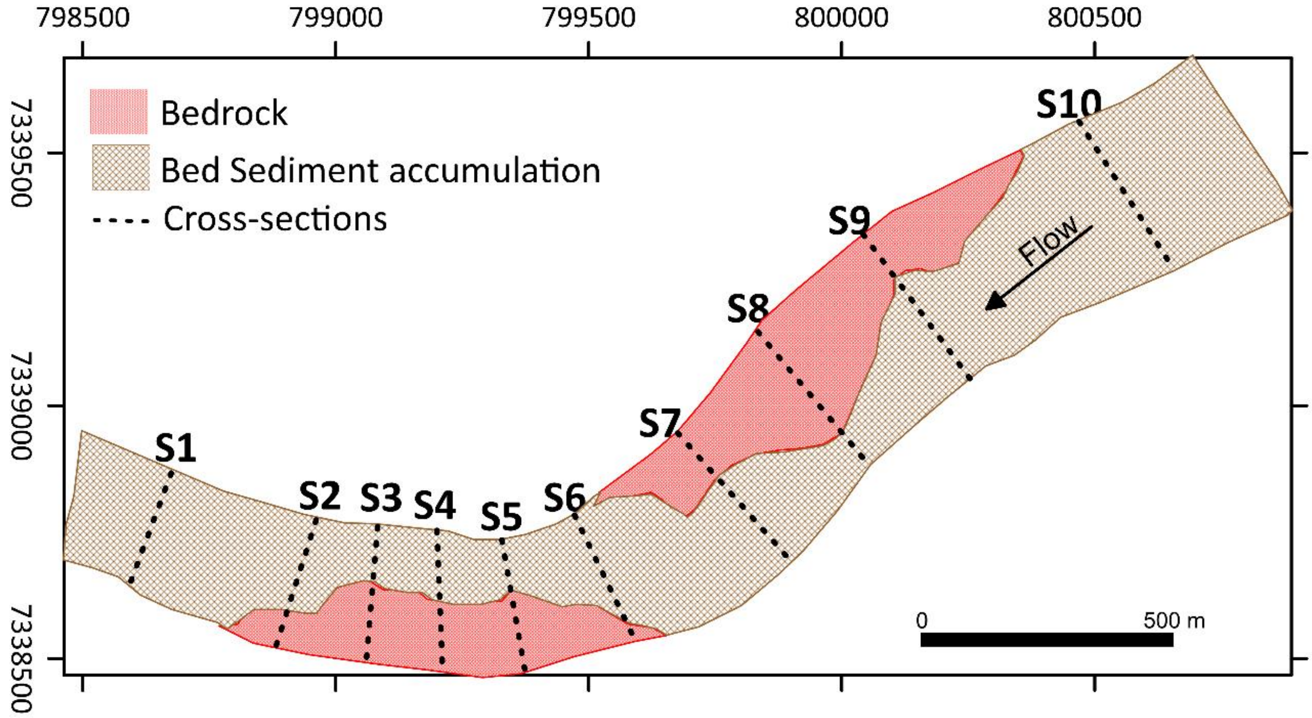


**Figure 8.** Distribution of bed sediment and two bedrock sectors: right bank upstream of the curve and left bank downstream.

The mapping of the bed material (Fig. 8) shows the upstream sector of the right bank and part of the curve, along with a downstream section of the left bank, formed by bedrock, indicating the complete removal of bed sediment due to the flow conditions during the campaign (Tab. 1). This condition triggers a slight increase in the concentration of suspended load downstream due to the secondary movements and helical cells of the curve, which alter the sediment concentration at different depths in this area of the channel and also contribute to the suspension of bed sediments and transport by the increased flow velocity downstream (Fig. 4). In the case studied, the flow dynamics influence the greater accumulation of bed sediments at the end of the channel stretch area (Fig. 8). Although not evaluated, under conditions of higher discharge energy from the Piquiri River and less effect of damming from the Paraná River, much of this accumulated sediment volume would likely be mobilized to the Paraná River. Otherwise, it would be inevitable for the system to become blocked, preventing the flow and discharge of the Piquiri River.

## 5. Conclusions

The study aimed to understand the sediment transport processes, flow dynamics, and morphology of a river bend in the Piquiri River. To this end, based on the bathymetric data of the bed, flow behavior, transport, and distribution of suspended and bed sediments in this bend of the Piquiri River, the following conclusions are drawn:

1. The bed morphology is more homogeneous in the upstream section, with an increase in depth starting from the river bend, primarily on the concave bank (left bank) due to bed excavation by secondary flow and helical cells, forming a scour hole at the location.
2. The flow is directed towards the left bank from upstream to downstream, being more pronounced at the curve location, where changes in flow velocity and discharge also occur, which are related to the channel morphology. The lower velocity at the curve is related to the flow dynamics in bed erosion and friction with the concave bank, caused by the water pressure gradient in the curvature. The curvature of the channel generates secondary flow, creating helical cells, which, in the case of extreme floods, triggers the detachment and transport of basalt blocks, unlike alluvial rivers where the process occurs even under ordinary flow conditions.
3. Comparing the flow distribution model of the studied curve with that of alluvial rivers, it is noticeable that in the latter, the roughness is significantly reduced compared to that of rocky rivers. This causes, in the studied case, the destruction of velocity cells and a rearrangement determined by local and specific conditions.
4. Although the average flow velocity is relatively homogeneous, the slight increase found in the downstream section is related to the local increase in slope due to the "knickpoint," which typically does not occur in curves of alluvial rivers.
5. There is variation in suspended sediments at different depths, as well as between the upstream and downstream sections. This condition is related to the influence of secondary flow and the increase in flow velocity from the curve to downstream.
6. Although the Css and MO at 150 cm are consistently higher than at 50 cm depth, the increase in Cs at 50 cm downstream of the curve results from the turbulent activity near the bed and the formation of secondary flows that act on the stirring and suspension of finer sediments transported by the flow.
7. The rocky characteristic of the bed prevents the formation of meanders in the final stretch of the Piquiri River; however, the curvature of the channel imposed by the litho-structure established a flow dynamic similar to meandering channels, with higher flow energy, the formation of vortices in the thalweg of the concave bank, and the redirection of the flow downstream to the left bank.
8. Some questions can be raised with the results of this study: a) The asymmetry of the curve section imposed by the litho-structure have as its most important factor the tilting of the blocks, or would hydraulic action be as important as in alluvial rivers? b) In the case of hydraulic contribution, what flow would provide sufficient specific power for the removal of the rocky material, and how frequently would this flow occur? c) Dating and facies analysis of the floodplain deposits could inform whether the channel's shift to the left bank could be reversed by endogenic (hydrosedimentary) processes, as observed in other rivers with similar conditions?

**Author´s contributions:** Altair Bennert: revision and editing, writing, fieldwork, methodology, data processing; José C. Stevaux: revision and editing, writing, methodology, data processing, supervision, financial acquisition; Geovani S. Lima: editing, writing, fieldwork; Isabel T. Leli: revision and editing, writing, fieldwork, methodology, data processing, supervision; Ericson H. Hayakawa: revision and editing, writing, fieldwork, methodology, data processing, supervision, project management, financial acquisition. All authors have read and agreed with the published version.

**Support:** We thank the National Council for Scientific and Technological Development (CNPq/Brazil) for the financial support provided to E. H. Hayakawa (process n°. 472012/2014-2 and 313757/2021-6), José C. Stevaux (process n°. 304863/2015-7 and 308957/2020), and Isabel T. Leli (Process n° 405190/2018-2) and "This study was partly funded by the Coordination for the Improvement of Higher Education Personnel – Brazil (CAPES) – Financial Code 001."

**Acknowledgments:** To Mr. Ademar da Silva for the support with field activities (loan and piloting of the vessel), to Dr. Leandro Luz for the field support, to Dr. Mário Luis Assine for the loan of the ADCP equipment, to Dr. Tony Vinícius Moreira Sampaio and Dr. Otávio Cristiano Montanher for their contributions to the statistical analyses, to the Laboratory of Environmental Dynamics Studies (LEDA) coordinated by Dr. Márcia Regina Calegari, and Dr. Vanessa Cristina dos Santos for their theoretical contributions.

**Declaration of competing interest:** The authors declare that there is no conflict of interest.

## References

1. BAGNOLD, R.A. Some aspects of river meanders**. U. S. Geological Survey Professional Paper** 282-E, 1960.
2. BALEK, J.; KOLAR. V., Statistical parameters of river bends. **Slovenk Akademia Bratislava**, Czecholovakia, v. 7, pp. 237-246, 1959.
3. BENNERT, A.; HAYAKAWA, E.H.; LELI, I.T.; STEVAUX, J.C. Morphology, flow structure, and sediment transport in the Paraná and Piquiri Rivers confluence, Brazil. **Revista Brasileira de Geomorfologia**. V 24, nº2, 2023. DOI: 10.20502/*rbg.v24i2.2337*.
4. BITTENCOURT, A.V.L. Sobre a quantificação do intemperismo na Bacia do Rio Piquiri – PR. **Boletim Paranaense de Geociências**, Curitiba, n.41, p.35-51, 1993.
5. CARVALHO, N. O. **Hidrossedimentologia prática.** Rio de Janeiro: CPRM, 1994.
6. CENDERELLI, D.A.; CLUER, B.L. Depositional Processes and Sediment Supply in Resistant-Boundary Channels: Examples from Two Case Studies. In: TINKER, K.; WOHL, E.E., Eds., **Rivers over Rock: Fluvial Processes in Bedrock Channels**, American Geophysical Union, Washington, DC, 1998.
7. CHARLTON, R. **Fundamentals of fluvial geomorphology.** New York: Routledge, 234p. 2007.
8. CHEN, D.; TANG, C. Evaluating secondary flows in the Evolution of sine-generated meanders. **Geomorphology**, 163-164, 2012, p. 37-44.
9. DANIELS, M.D.; RHOADS, B.L. Influence of a large woody debris obstruction on three-dimensional flow structure in a meander bend. **Geomorphology**, 51, 2003, p. 159-173.
10. DURY, G.H., The shrinkage of Warwickshire Itchen. **Conventry of Natural History and Science Society Proceedings**, v. 2, pp. 208-214, 1953.
11. DORNELLES, A.M. **Utilização de um perfilador acústico de correntes por efeito Doppler (ADCP) para a estimativa da concentração de sedimentos em suspensão (CSS)**. Dissertação (Mestrado em Engenharia) –Programa de Pós-graduação em Recursos Hídricos e Saneamento Ambiental, Universidade Federal do Rio Grande do Sul (UFRGS), Porto Alegre, 2009. 126p.
12. ENGEL, F.L. **The Fluvial Dynamics of Compound Meander Bends**. Illinois, 2004. 187p. Tese (Doutorado em Geografia) - Universidade de Illinois, 2014.
13. ENGEL, F.L.; JACKSON, P.R. The Velocity Mapping Toolbox. User guide for version 8.08. **USGS Science for a changing world**, 2016.
14. FORTES, E.; STEVAUX, J.C.; VOLKMER, S. Neotectonics and channel evolution of the lower Ivinhema River. A right-bank tributary of the upper Paraná River, Brazil. **Geomorphology**, v. 70, p. 325-338, 2005.
15. FRANCO, A.L.A.; ETCHBEHERE, M.L.C.; STEVAUX, J.C. Hipótese sobre os condicionantes neotectônicos do barramento natural da foz do rio Ivaí (PR) com base em levantamento ecobatimétrico. **Revista Geociências UnG,** v. 7. n. 1, p. 78-86, 2008.
16. FULFARO, V.J.; SAAD, A.R.; SANTOS, M.V.; VIANNA, R.B. Compartimentação e evolução tectônica da Baciado Paraná. **Revista Brasileira de Geociências**, v. 12. n. 4, p. 590-611, 1982.
17. GÜNERALP, I., ABAD, J.D., ZOLEZZI, G., HOOK, J. Advancing and challenges in meandering channels research. **Geomorphology**, v. 163-164, 2012.
18. GUERRERO, M.; RUTHER, N.; SZUPIANY, R.; BARANYA, S.; LATOSINSKI, F. The Acoustic Properties of Suspended Sediment in Large Rivers: Consequences on ADCP Methods Applicability. **Water**, 8, 13; DOI:10.3390/w8010013, 2016.
19. KASVI, E.; VAAJA, M.; KAARTINEN, H.; KUKKO, A.; JAAKKOLA, A.; FLENER, C.; HYYPPA, J.; OLHO, P. Sub-bend scale flow-sediment interaction of meander bends – A combined approach of field observations, close- range sensing and computational modeling. **Geomorphology**, 238, 2015, p. 119-134.
20. KAYVANTASH, D.; COJAN, L.; KISSEL, C.; FRANKE, C. Magnetic fingerprint of the sediment load in meander bend section of the Seine River (France). **Geomorphology**, 286, 2017, p. 14-26.
21. KONSOER, M.K.; RHOADS, B.L.; BEST, J.L.; LANGENDOEN, E.J.; ABAD, J.D.; PARSONS, D.R.; GARCIA, M.H. Three-dimensional flow structure and bed morphology in large elongate meander loops with different outer bank roughness characteristics. **Water Resources Research**, 52, 2016, p.9621-9641.
22 LATRUBESSE, E.M.; KALICKI, T. Late Quaternary Paleohydrology of the Purus River, Amazon, Brazil. **Zeitschrift Fur Geomorphologie**, Tubingem, Alemanha, v. 129, p. 41-59, 2002.
23. LATOSINSKI, F. G; SZUPIANY, R. N; GARCIA, C.M; GUERRERO, M; AMSLER, M.L. Estimation of concentration and load of suspended bed sediment in large river by means of acoustic doppler technology. **Journal of Hydraulic Engineering**, 2014.

24. LELI, I.T; STEVAUX, J.C.; NÓBREGA, M.T. PRODUÇÃO E TRANSPORTE DA CARGA SUSPENSA FLUVIAL: TEORIA E MÉTODO PARA RIOS DE MÉDIO PORTE. **Bol. geogr. Maringá**, v. 28, n. 1, p. 43-58, 2010.
25. LELI, I.T.; STEVAUX, J.C. Lake-island: A distinct morphology of river systems. **Journal of South American Earth Sciences**. V111, 2021.
26. LELI, I.T., STEVAUX, J.C., 2022. The polygenetic floodplain of the Upper Paraná River**. J. S. Am. Earth Sci**. 119, 103985 DOI: 10.1016/j.jsames.2022.103985.
27. LEOPOLD, L.B.; WOLMAN, M.G., River channel pattern; braided meandering and straight. **U. S. Geological Survey Professional Paper** 282-D, 1957.
28. LEOPOLD, L.B.; WOLMAN, M.G., River Meanders. **Geological Sociatey American Bulletin**, v. 71, pp. 769-794, 1960.
29. LEOPOLD, L.B.; WOLMAN, M.G., Miller, J.P., **Fluvial Processes in Geomorphology**, Dover Publications, INC, New York, 1964.
30. LIMA. A.G.; BINDA, A.L.,Lithologic and structural controls on fluvial knickzones in basalts of the Paraná Basin, Brazil. **Journal of South American Earth Sciences,** 48:262-270, 2013.
31. LIMA, J.E.F.W.; Lopes, W.T.A.; SILVA, E.M.; VIEIRA, M.R. Diagnóstico hidrossedimentológico da Bacia do Rio Piquiri. – Planaltina, DF: **Embrepa Cerrados**, 2004. 25p. (Boletim de pesquisa e desenvolvimento/Embrapa Cerrados, ISSN 1676-918;134).
32. LUZ, L.D. STEVAUX, J.C., PAROLIN, M., SILVA, A. Alteração hidrodinâmica em rios meandrantes: Caso do rio Cuiabá, Pantanal. In: VIII Simpósio Regional sobre Hidráulica de Ríos, Cordoba, Argentina, 2017.
33. LUZ, L.D.; SZUPIANY, R. N.; PAROLIN, M.; SILVA, A.; STEVAUX, J.C. Obtuse-angle vs. Confluence sharp meandre bends: insights from the Paraguay-Cuiabá confluence in the Pantanal wetlands, Brazil. **Geomorphology**, 2020.
34. MAACK R. **Geografia física do Estado do Paraná**. Curitiba, Banco BADEP, UFPR, IBPT. 1968, 350p.
35. MARTINEZ, M.; HAYAKAWA, E.H.; STEVAUX, J.C.; PROFETA, J.D. SL index as indicator of anomalies in the longitudinal profile of the Pirapó River. **Geociências UNESP**, São Paulo, v. 30, n. 1, p 63-76, 2011.
36. MILLER, J.R. The influence of bedrock geology on knickpoint development and channel-bed degradation along downcutting stream in south-central Indiana. **J. Geol**., 99:591-605, 1991.
37. MILLER, J.R.; CLUER, L.B. Modeling considerations for simulation of flow in bedrock channels. In: TINKER, K.; WOHL, E.E., Eds., **Rivers over Rock: Fluvial Processes in Bedrock Channels**, American Geophysical Union, Washington, DC, 1998.
38. MINEROPAR- Minerais do Paraná S.A. **Atlas Geomorfológico do Estado do Paraná**. Universidade Federal do Paraná, Curitiba, 2006.
39. MORISAWA, M. **Stream, their dynamics and morphology**. New York: McGraw- Hill Boock Company, 1968. 175 p.
40. ORFEO, O. 1995. **Sedimentología del río Paraná en el área de suconfluencia con el río Paraguay. Facultad de Ciencias Naturales y Museo, Universidad Nacional de LaPlata**, Tesis Doctoral, 289 p.
41. PAES, R., STEVAUX, J.C., ETCHEBEHERE, M.L.C., LELI, I.T., 2008. Dinâamica e morfologia do canal de confluência dos rios Paraná e Paranapanema pelo método do mapeamento temporal. **Geografia**, Londrina 17, 37–47. http://www.uel.br/revistas/geografia.
42. PAROLIN, M.; GUERREIRO, R.L.: KUERTEN, S.; MENEZES, H.R. Bacias hidrográficas paranaenses. In. PAROLIN, M.; VOLKMER-RIBEIRO, C.; LENADRINI, J.A. (Org). **Abordagem ambiental interdisciplinar em bacias hidrográficas no Estado do Paraná**. Campo Mourão: Ed. Fecilcam, 2010, p. 59-104.
43. PARSONS, D.R.; JACKSON, P.R.; CZUBA, J.A.; ENGEL, F.L.; RHOADS, B.L.; ORBERG, K.A.; BEST, J.L; MUELLER, D.S.; JOHNSON, K.K.; RILEY, J.D. Velocity Mapping ToolBox (VMT): a processing and visualization suite for moving-vessel ADCP measurements. **Earth Surface Processes and Landforms**, v. 38, p. 1244-1260, 2013.
44. PIRES NETO, A.G; BARTORELLI, A.; VARGAS. M.S. A planície do rio Paraná. **Boletim Paranaense de Geociências**, 42, 217-229, 1994.
45. RAMONELL, C.G.; AMSLER, M.L.; ORFEO, O.; MONTAGNINI, M.D.; PEREZ, M. Ajustes morfológicos-sedimentários del río Bermejo em torno al puente Lavalle (Chaco Argentino). **Tecer Simpósio Regional sobre hidráulica de rios**, UNC, 2007.
46. REMOR, M.B.; SAMPAIO, S.C.; DAMATTO, S.R.; CASTILHOS, Z.C.; STEVAUX, J.C.; VILAS BOAS, M. A.; DOS REIS, R. R. Geochemistry of the Upper Paraná River floodplain: study of the Garças Pond and Patos Pond. **Journal of Radioanalytical and Nuclear Chemistry,** v. 305, p. 409-418, 2015.
47. ROSOVSKII, J.L. 1957. Flow of water in bends of open channels. In: **Academy of Sciences of the Ukrainian SSR**; Kiev [ translated from Russian by the Israel Program for Scientific Translations, Jerusalem, 1961].

48. SANTOS, M.D, STEVAUX.; J.C, GASPARETTO, N.V.L.; SOUZA FILHO. E.E. Geologia e geomorfologia da planície aluvial do rio Ivaí-PR. **Revista Brasileira de Geomorfologia**,v. 1, p. 23-34, 2008.
49. SANTOS, V.C.; STEVAUX, J.C.; SZUPIANY, R.N. Confluence analysis at basin scale in a tropical bedrock river - The Ivaí River, Southern Brazil. **Journal of South American Earth Sciences**, v. 116, p. 103877, 2022.
50. SOUZA JR.; M.D.; SOUZA, M.L.; SALAMUNI, E.; STEVAUX, J.C.; MORALES, N. Análise morfotectônica da bacia hidrográfica do rio Ivaí-PR, curso inferior. **Revista Brasileira de Geomorfologia**, v.14, n.2, (Abr-Jun) p.213-220, 201v. 2013.
51. STEVAUX, J.C. The Upper Paraná River (Brazil): geomorphology, sedimentology and paleoclimatology. **Quaternary International**, Londres, v 21, p.143-161, 1994.
52. STEVAUX, J.C.; SOUZA, I. Floodplain construction in an anastomose driver. **Quaternary International**, Amsterdan, v. 114, p.55-66, 2004.
53. STEVAUX, J.C.; PAES, R.; FRANCO, A.A.; ETCHEBEHERE, M.L.; FUJITA, R.H. Morphodynamics in the confluence of large regulated rivers: the case of Paraná and Paranapanema Rivers. **Latin American Journal of Sedimentology and Basin Analysis**, v. 16, p. 101-109, 2009.
54. STEVAUX, J. C.; LATRUBESSE, E. M. Iguazu Falls: A history of differentialfluvial incision. In: Piotr Migon. (Org.). Geomorphological landscapes of the world. Londres: Springer, 2010, v., p. 102-110.
55. STEVAUX, J.C.; LATRUBESSE, E.M. **Geomorfologia Fluvial**. Oficina de Textos. São Paulo, 2017.
56. STEVAUX, J.C.; GON, P.P., LELI, I.T.; FUJITA, R.H. Why do large rivers tend to form multichannel? A field study in the Upper Paraná River. **Revista Brasileira de Geomorfologia**, v. 22, p. 967-985, 2021.
57. SUGUIO, K. Introdução à sedimentologia. Edgard Blucher, Ed. da Universidade de São Paulo. 1973.
58. SUGUIO, K.; BIGARELLA, J.J. **Ambiente Fluvial**. Associação de Defesa e Educação Ambiental (ADEA), Curitiba: Editora da Universidade Federal do Paraná, 1979.
59. SZUPIANY, R.N.; AMSLER, M.L.; PARSONS, D.R.; BEST, J.L. Morphology, flow structure, and suspended bed sediment transport in two large braid-bar confluences. **Water Resources Research**, v. 45, 2009.
60. SZUPIANY, R.N.; AMSLER, M.L.; HERNANDEZ, J.; PARSONS, D.R.; BEST, J.L.; FORNARI, E.; TRENTO, A. Flow fields, bed shear stresses, and suspended bed sediment dynamics in bifurcations of a large river. **Water Resources Research**, v. 48, p. 1-20, 2012.
61. TIRON, L. J.; COZ, J. L.; PROVANSAL, M.; PANIN, N.; RACCASI, G.; DRAMAIS, D.; DUSSOUILLEZ, P. Flow and sediment processes in a cutoff meander of the Danube Delta during episodic flooding. **Geomorphology**, 106, 2009, p. 186-197.
62. TUROWSKI, J. M.; HOVIUS, N.; HSIEH, M. L.; LAGUE, D.; CHEN, M. C. Distribution of erosion across bedrock channels. **Earth Surf. Proc. Land**., 33, 353–363,2008, DOI: 10.1002/esp.1559.
63. WEIBEL, C. L.; SZUPIANY, R.; LATOSINSKI, F.; AMSLER, M.; REPASCH, M. Sources and temporal dynamics of suspended sediment transport along the Paraná River system. **Journal of South America Earth Science**, v. 1, p. 1-13, 2022. DOI: 10.1016/j.jsames.2022.103968.
64. WHIPPLE, K.X., Beyond bedrock river process and form. In, THINKLER, K.J.; WOHL, E.E. (Eds.) Rivers over Rock – Fluvial processes in bedrock channels. P. 35-60, **American Geophysical Union**, Washington, DC, 1998.
65. YOUSEFI, S.; POURGHASEMI, H. R.; HOOKE, J.; NAVRATIL, O.; KIDOVÁ, A. Changes in morphometric meander parameters identified on the Karoon River, Iran, using remote sensing data. **Geomorphology**, 271, 2016, p.55-64.